WILEY

Online Proofing System Instructions

The Wiley Online Proofing System allows proof reviewers to review PDF proofs, mark corrections, respond to queries, upload replacement figures, and submit changes directly from the locally saved PDF proof.

1. For the best experience when reviewing your PDF proof ensure you are connected to the internet. This will allow the locally saved PDF proof to connect to the central Wiley Online Proofing System server. If you are connected to the Wiley Online Proofing System server you should see a green check mark icon above in the yellow banner.

Connected Disconnected

2. Please review the article proof on the following pages and mark any corrections, changes, and query responses using the Annotation Tools outlined on the next 2 pages.

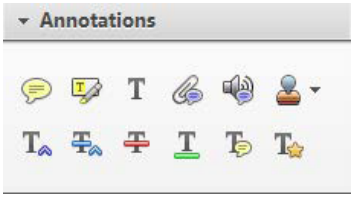

3. Save your proof corrections by clicking the "Publish Comments" button in the yellow banner above. Corrections don't have to be marked in one sitting. You can publish comments and log back in at a later time to add and publish more comments before you click the "Complete Proof Review" button below.

4. If you need to supply additional or replacement files bigger than 5 Megabytes (MB) do not attach them directly to the PDF Proof, please click the "Upload Files" button to upload files:

Upload files

Click Here

5. When your proof review is complete and all corrections have been published to the server by clicking the "Publish Comments" button, please click the "Complete Proof Review" button below:

IMPORTANT: Did you reply to all author queries found on the first page of your proof?

IMPORTANT: Did you click the "Publish Comments" button to save all your corrections? Any unpublished comments will be lost.

IMPORTANT: Once you click "Complete Proof Review" you will not be able to add or publish additional corrections.

Complete Proof Review

Click Here

WILEY

Author Query Form

Journal: PC

Article: 24774

Dear Author,

During the copyediting of your manuscript the following queries arose.

Please refer to the query reference callout numbers in the page proofs and respond to each by marking the necessary comments using the PDF annotation tools.

Please remember illegible or unclear comments and corrections may delay publication.

Many thanks for your assistance.

Query References	Query	Remarks?
AQ1	AUTHOR: Please check whether the edit made to the title is OK as set.	
AQ2	AUTHOR: Please provide department/division, university/institute names for the affiliations where required. Also check whether all the affiliations are OK as typeset.	
AQ3	AUTHOR: Please provide expansion for DGEBA, TGA in first occurrence if necessary.	
AQ4	AUTHOR: Please confirm that given names (red) and surnames/family names (green) have been identified correctly.	

New Epoxy Composite Thermosets with Enhanced Thermal Conductivity and High T_g Obtained by Cationic Homopolymerization

Isaac Isarn,[1] Francesco Gamardella,[2] Lluís Massagués,[3] Xavier Fernàndez-Francos,[4] Àngels Serra,[2] Francesc Ferrando[1]

[1]*Department of Mechanical Engineering, Universitat Rovira i Virgili, Tarragona 43007, Spain*

[2]*Department of Analytical and Organic Chemistry, Universitat Rovira i Virgili, Tarragona 43007, Spain*

[3]*Department of Electronic, Electric and Automatic Engineering, Universitat Rovira i Virgili, Tarragona 43007, Spain*

[4]*Thermodynamics Laboratory, ETSEIB, Universitat Politècnica de Catalunya, Barcelona 08028, Spain*

Thermal dissipation is a critical aspect for the performance and lifetime of electronic devices. In this work, novel composites based on a cycloaliphatic epoxy matrix and BN fillers, obtained by cationic curing of mixtures of 3,4-epoxy cyclohexylmethyl 3,4-epoxy cyclohexane carboxylate (ECC) with several amounts of hexagonal boron nitride (BN) were prepared and characterized. As cationic initiator a commercial benzylanilinium salt was used, which by addition of triethanolamine, exhibited an excellent latent character and storage stability. The effect of the formulation composition was studied by calorimetry and rheological measurements. The variation of thermal conductivity, thermal stability, thermal expansion coefficient, and thermomechanical and mechanical properties of the composites with the load of BN filler (ranging from 10 to 40 wt%) was evaluated. An improvement of an 800% (1.04 W/m·K) in thermal conductivity was reached in materials with glass transition temperatures >200°C without any loss in electrical insulation. POLYM. COMPOS., 00:000–000, 2018. © 2018 Society of Plastics Engineers

INTRODUCTION

The use of high frequencies in electronic devices, with a great electric current, leads to an increase in their temperature caused by the Joule effect. Limiting their work temperature favors their performance, lifetime and reliability and therefore the thermal management of these materials has become an important issue [1]. To dissipate the heat produced during their operation, thermal conductive materials are required and, since many parts of the devices are usually coated or packaged with epoxy resins, which are thermal insulators, the increase in their thermal conductivity is of utmost importance [2]. Epoxy thermosets are widely used because of the versatility in their properties [3, 4]. They are used in electrical and electronic applications because of their good compatibility with a large variety of materials, high electrical insulation and good thermal, corrosion and chemical resistance [5]. However, epoxy thermosets exhibit poor thermal conductivity, in the range 0.1–0.3 W/m·K. The addition of thermal conductive but electrically insulating fillers to the resin is one of the easiest methods for effectively dissipating heat in such devices at the lowest price. In last years, many efforts and studies have been intended to increase the thermal conductivity of these resins, emphasizing the great importance of this subject [6–9]

Cycloaliphatic epoxy resins are preferred in electronic applications for their low viscosity, which permit to impregnate zones with small and abrupt morphology. They have excellent weathering and electrical performance with a low dielectric loss and high electrical resistivity, up to or above their glass transition temperatures, which provide high performance and reliability in both AC and DC circuitry. Their inherent low viscosity enables them to be formulated with higher levels of inorganic fillers, which enhances mechanical and electrical track resistance for electric materials. According to that, in the present study we have selected 3,4-epoxy cyclohexylmethyl 3,4-epoxy cyclohexane carboxylate (ECC) as epoxy monomer. Cycloaliphatic epoxy resins are mainly

Correspondence to: F. Ferrando; e-mail: f.ferrando@urv.cat
DOI 10.1002/pc.24774
Published online in Wiley Online Library (wileyonlinelibrary.com).

cured with anhydrides, which show some drawbacks such as toxicity, sensitivity to humidity, yellowing, high viscosities or too short pot life that are serious problems for electronic applications that require high working temperatures [10]. As an alternative, cationic ring-opening polymerization was studied and developed intensively, since the stereoelectronic nature of the epoxy group lead to an extremely low reactivity towards common nucleophilic crosslinkers [11]. Among the cationic curing agents, amino complexes of BF_3 can be used with a moderate latency at room temperature but the electrical properties of cured resins tend to deteriorate at high temperature and high humidity [12]. Lanthanide triflates were also proposed, but the T_gs of the cured materials were lower, although the enthalpy evolved during curing was higher [13]. Endo's group has been one of the major contributors to the field of latent thermal initiators and they observed that the activity can be effectively controlled through the change of electronic and steric properties of the substituents and varying the nucleophilicity of the counteranion in onium salts [14, 15]. Among thermal latent initiators, sulfonium, ammonium, phosphonium and hydrazinium salts were reported [11]. In this study, a commercial anilinium salt, N-(4-methoxybenzyl)-N,N-dimethylanilinium hexafluoroantimonate [16], which to the best of authors' knowledge had not been previously reported to be used to crosslink cycloaliphatic epoxy resins, was selected as initiator and modified with triethanolamine (TEA) to reach a high latency. Many latent systems already exist for cycloaliphatic epoxy resins [17, 18] but generally, they are photochemically activated, which limits their use to the preparation of thin coatings and present some drawbacks in the curing of shadowy parts.

As filler, we selected hexagonal boron nitride (h-BN), which has gained great popularity in recent years in the field of high thermal conductivity. This is due to the combination of properties: high thermal conductivity in planar direction, good dielectric properties, low thermal expansion coefficient (CTE) and density below other kind of particles [19, 20]. We recently studied similar curing processes based on a DGEBA resin [7]. The low viscosity and the higher reactivity of cycloaliphatic epoxides towards cationic initiators, together with the compact structure, are expected to be advantageous to get highly crosslinked materials with high T_g and thermal conductivity. The mechanical and thermal properties of BN composites have been determined by thermogravimetric and thermomechanical analysis (TMA). Mechanical properties such as hardness or adhesion were also tested. Electrical resistivity and thermal conductivity were also measured.

MATERIALS AND METHODS

Materials

ECC (ERL-421D, EEW = 126.15 g/*Eq*. was provided by Dow Chemical Company. Initiator CXC1612 from King Industries Inc., USA, which was determined to be N-(4-methoxybenzyl)-N,N-dimethylanilinium hexafluoroantimonate, was solubilized in propylene carbonate at 50 wt%. Propylene carbonate and TEA were provided by Sigma-Aldrich and purified by distillation. Platelets of h-BN were supplied by ESK Ceramics GmbH, TPC 006, with an average particle size of 6 μm in length (Fig. 1). F1

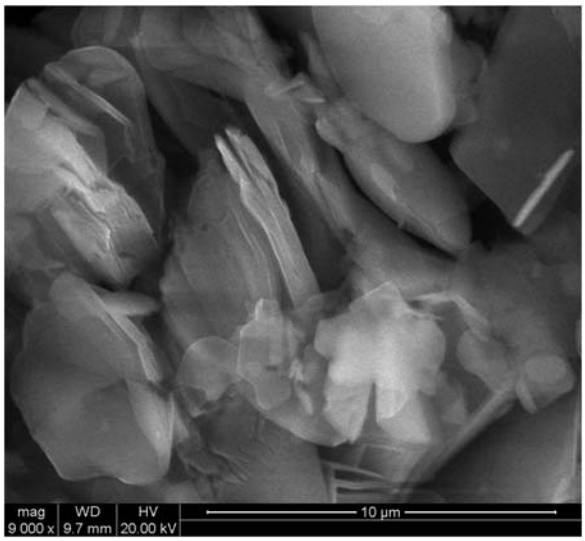

FIG. 1. ESEM micrographs of the BN particles used in the study.

Sample Preparation

The mixtures were prepared by mixing ECC with 1 phr (parts of initiator per hundred parts of resin) and 0.1 phr of TEA. For composite samples, the required amount of BN was added in wt% to the previous formulation. The mixtures were manually stirred until homogeneity (10 min) and degassed under vacuum to prevent the appearance of bubbles during the curing process. Finally, the samples were poured onto aluminum molds and cured following a multistep temperature schedule at 100, 120, 150, 180 and 200°C, with a dwelling time of 1 hour at each temperature.

Characterization Techniques

A differential scanning calorimeter (DSC) Mettler DSC-821e calibrated using an In standard (heat flow calibration) and an In-Pb-Zn standard (T calibration) was used to study the cure. Samples of approximately 5–10 mg were tested in aluminum pans with a pierced lid in N_2 atmosphere with a gas flow of 100 mL/min. The dynamic studies were performed between 30 and 250°C with a heating rate of 10°C/min. The reaction enthalpy (Δh) was integrated from the calorimetric heat flow signal (dh/dt) using a straight baseline, with the help of the STARe software.

Rheometric measurements were carried out in a TA Instruments AR G2 rheometer, equipped with electrical

heated plates. Parallel plate geometry (25-mm diameter disposable aluminum plates) was used. Complex viscosity (η^*) and viscoelastic properties of the mixtures were recorded as function of angular frequency ω (rad/s) in the range of linear viscoelasticity, obtained from constant shear storage modulus (G') in a strain sweep experiment at 1 Hz at 30°C.

The thermal stability of cured samples was determined using a Mettler TGA/SDTA 851e thermobalance under inert atmosphere (N_2 at 100 mL/min) and Mettler Toledo TGA/DSC 1 under air (synthetic air at 50 mL/min). Pieces of cured samples of 10–15 mg were degraded between 30 and 600°C at a heating rate of 10°C/min. Dynamic mechanical thermal analyses (DMTAs) were performed with a TA Instruments DMA Q800 analyzer. Prismatic rectangular samples (15 × 6 × 2.3 mm^3) were analyzed by trhee-point bending at a heating rate of 3°C/min from 35 to 300°C using a frequency of 1 Hz and oscillation of 0.1% of sample deformation. The Young modulus (E) was determined at 30°C as explained in a previous paper [7]. TMAs were carried out on a Mettler TMA40 thermomechanical analyzer. Cured samples (12 × 12 × 2.3 mm^3) were supported by the clamp and one silica disc to distribute uniformly the force and heated at 5°C/min from 35 to 150°C by application of a force 0.01 N, a minimum force to avoid distortion of the results [7].

Knoop microindentation hardness was measured as reported before with a Wilson Wolpert 401 MAV device following ASTM D1474-13 [7]. For each material a minimum of 20 determinations were made with a confidence level of 95%. Adhesion tests of different mixtures on rectangular steel plates were done as previously reported [7] by tensile lap-shear strength of bonded assemblies using a Houndsfield H10KS universal test machine with 10 kN load cell, following ASTM D1002-10 method. At least seven samples were tested for each mixture. Surface fracture was examined with a FEI Quanta 600 environmental scanning electron microscope (ESEM) that allows collecting electron micrographs at 10–20 kV and low vacuum mode of uncoated specimens with low electron conductivity.

X-ray diffraction (XRD) measurements were made using a Siemens D5000 diffractometer (Bragg-Bretano parafocusing geometry and vertical Θ-Θ goniometer) fitted with a curved graphite diffracted-beam monochromator, incident and diffracted-beam Soller slits, a 0.06° receiving slit and scintillation counter as a detector. The angular 2Θ diffraction range was between 5 and 70°. The data were collected with an angular step of 0.05° at 3 s per step and sample rotation. $Cu_{k\alpha}$ radiation was obtained from a copper X-ray tube operated at 40 kV and 30 mA.

Volume resistivity of samples was measured on a Megohmmeter Burster model 24508 insulation tester at room temperature following ASTM D257-14 as reported before [7]. Pieces of 12 × 12 × 2.3 mm^3 were essayed between two stainless steel electrodes with an area of 19.635 mm^2 each one. The applied voltage to the thermosetting composites was 500 V during 1 min. Thermal conductivity was measured using the Transient Hot Bridge method by a THB 100 device from Linseis Messgeraete GmbH. A HTP G 9161 sensor was used with a 3 × 3 mm^2 of area calibrated with polymethyl methacrylate (PMMA), borosilicate crown glass, marble, Ti-Al alloy and titanium. Two equal polished rectangular samples (12 × 12 × 2.3 mm^3) were placed in each one of the faces of the sensor. Due to the small size of sensor, side effect can be neglected. A measuring time of 100 s with a current of 10 mA was applied to each of the five measures done for the different formulations.

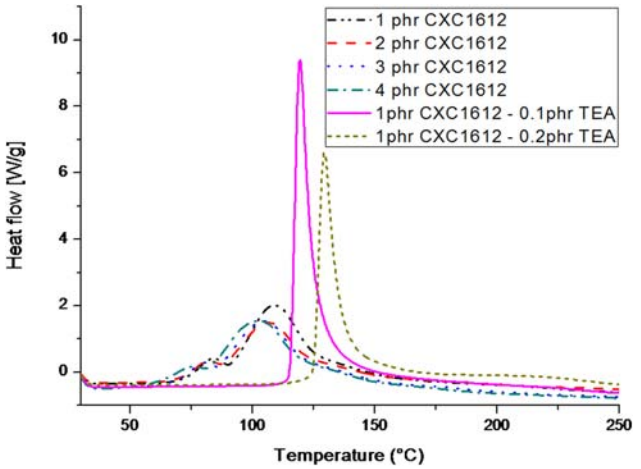

FIG. 2. DSC scans of ECC formulations with several proportions of initiator and amine. [Color figure can be viewed at wileyonlinelibrary.com]

COLOR ONLINE AND BW IN PRINT

RESULTS AND DISCUSSION

Optimization of the Curing Process of the Neat and BN Filled Formulations

Initiators play an important role in the curing of epoxies mainly for two reasons: they have a catalytic effect and decrease the activation energies accelerating the reaction, and give to thermosets specific properties. The choice of cationic initiators with low-nucleophilicity counter-anions can significantly enhance the reactivity of cationic curing systems [21]. In this study, we have selected as initiator the commercial compound, CXC1612, which by NMR spectroscopy was disclosed to be N-(4-methoxybenzyl)-N,N-dimethylanilinium hexafluoroantimonate [15]. However, this cationic curing system has not been reported so far in cycloaliphatic epoxies.

To study the curing process of ECC with CXC1612, different amounts of initiator were tested, from 1 to 4 phr. Fig. 2 shows the dynamic calorimetric curves for the formulations studied. The main data extracted from DSC are shown in Table 1. F2 T1

The figure shows that on increasing the proportion of initiator the exotherm shifts at lower temperature because

TABLE 1. Calorimetric data from formulations with some proportions of initiator and TEA.

Initiator (phr)	TEA (phr)	T_{onset}[a] (°C)	T_{peak}[b] (°C)	Δh[c] (J/g)	Δh[c] (kJ/ee)
1	0	87	109	596	75
2	0	83	107	571	72
3	0	80	105	569	71
4	0	77	103	599	76
1	0.1	116	119	698	88
1	0.2	125	129	541	68

[a]Onset temperature of the exothermic curve.
[b]Temperature of the maximum of the peak of the curing exotherm.
[c]Enthalpy of the curing process by gram of mixture or by epoxy equivalent.

TABLE 2. Calorimetric data of formulation after various times to be prepared.

Time	T_{peak}[a] (°C)	Δh[b] (J/g)	Δh[b] (kJ/ee)
First day	119	698	88
1 week	118	691	87
4 weeks	118	683	86
6 weeks	117	675	85
8 weeks	117	673	85
12 weeks	117	670	84
16 weeks	116	660	83

[a]Temperature of the maximum of the peak of the curing exotherm.
[b]Enthalpy of the curing process by gram of mixture or by epoxy equivalent.

of the catalytic effect. The enthalpy released, given in Table 1, is similar for all the formulations in spite of the amount of initiator. It is worth noting that the curves are quite complex with two broad and partially overlapped exotherms probably due to the different polymerization mechanisms: activated monomer and activated chain end, which are competitive in cationic systems [22]. Moreover, the curing starts at low temperature, which can lead to a premature curing and too short pot life.

To reduce these drawbacks we added small proportions of TEA to the formulation, since it has been reported that it is an efficient inhibitor of low temperature polymerization in cationic systems [23]. The addition of TEA to formulations with 1 phr of initiator leads to curves with a sharp and narrow shape, starting a fast reaction at high temperature, which is characteristic of latent curing systems. Moreover, the addition of 0.1 phr of TEA produces an increase of the heat evolved during curing up to 88 kJ/ee, but a further increase of the amount of inhibitor, which act as a poison for the cationic curing, shifted the curing onset to higher temperatures but this delay in the curing process resulted in incomplete cure. Therefore, we selected as the best catalytic system the mixture of ECC with 1 phr of CXC1612 and 0.1 phr of TEA.

Once selected the base formulation, we performed periodic DSC scans to evaluate the stability of the mixture stored at room temperature. The curves were almost overlapped confirming the excellent stability of the system. The mixture perfectly preserves the latent characteristic and has a minimal diminution of the temperature peak (see Table 2). After four months stored at room temperature, only a loss of 6% of the curing enthalpy was observed. The mixture also kept the same viscosity during this period, without any sign of polymerization. Then, it can be confirmed that this optimized curing system may be advantageous for industrial applications, since in addition to the instantaneous curing at the triggering temperature, the mixtures can be easily stored for long time without loss in their characteristics.

In order to improve the thermal conductivity and to evaluate the effect on the different characteristics of the composites, different percentages of BN were added to the epoxy formulation. The maximum proportion of BN added to the formulation was 40 wt%, since higher amounts of filler increased the viscosity of the formulation too much and generated big difficulties to prepare homogeneous mixtures. It should be commented that in the previous study, based on DGEBA resins, the maximum amount of BN added was only 20 wt% because of the higher viscosity of DGEBA resin. The curing evolution of the formulations was investigated by DSC, as shown in Fig. 3.

It can be observed that on increasing the proportion of filler there is a decrease in the height of the exotherms, indicating a diminution in the curing rate. However, the shape of the curves is similar, confirming that the latency is kept unaltered. The heat released decreases from 88 to 68–69 kJ/ee (see Table 3) on adding BN to the formulation but an increase in the proportion no longer affects the released enthalpy. Thus, from the point of view of the curing mechanism it can be stated that BN has an inert character in the cationic homopolymerization. Nevertheless, it affects the final curing degree achieved in dynamic DSC experiments, probably due to topological restrictions caused by the BN particles, which can hinder the growing of the polymer chain, leading to a decrease of the curing enthalpy.

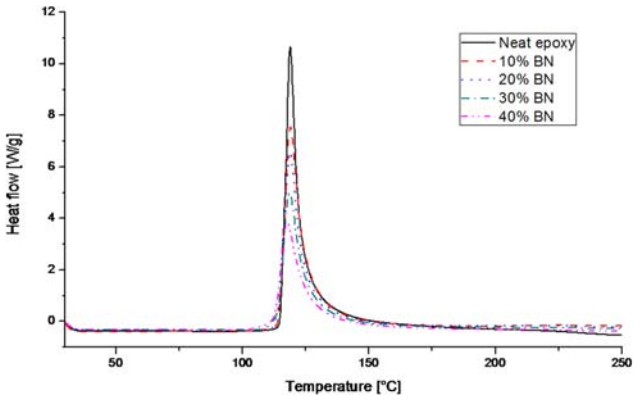

FIG. 3. DSC scans of formulations with several proportions of BN in wt%. [Color figure can be viewed at wileyonlinelibrary.com]

COLOR ONLINE AND BW IN PRINT

DOI 10.1002/pc

TABLE 3. Calorimetric data on varying the BN proportion in ECC formulation with 1 phr of initiator and 0.1 phr of TEA.

% BN (in weight)	% BN (in volume)	T_{peak}[a] (°C)	Δh[b](J/g)	Δh[b] (kJ/ee)
0	0	119	698	88
10	5.6	119	488	69
20	11.7	119	436	68
30	18.9	119	378	68
40	26.0	118	330	69

[a]Temperature of the peak of the curing exotherm.
[b]Enthalpy of the curing process by gram of mixture or by epoxy equivalent.

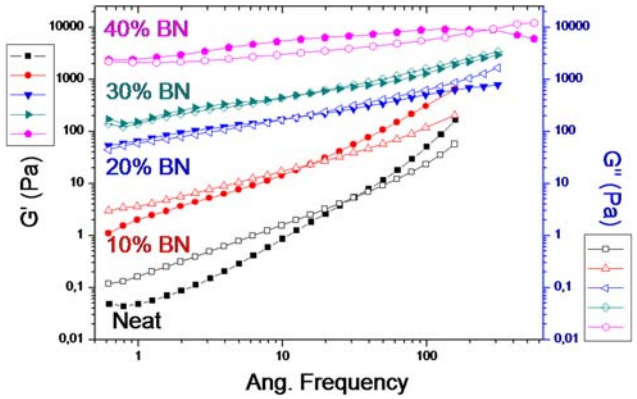

FIG. 5. Plots of G' (filled) and G'' (open symbols) against ω of uncured formulations at 30°C. [Color figure can be viewed at wileyonlinelibrary.com]

COLOR ONLINE AND BW IN PRINT

Rheological Study of the Formulations

Rheological analysis provides important information on the evolution of the structure and consequently, on the interaction between the filler and matrix. Viscosity is the most important property affecting the applicability of encapsulation resins. For this reason, measurements of viscosity are essential for understanding the processability, to control and optimize process conditions and product performance [24]. Thus, the formulations were studied by performing oscillatory experiments to determine their viscoelastic response.

To determine viscoelastic constants in this kind of mixtures we must firstly establish the linear viscoelastic region (LVR) or Newtonian range to work on it, which means a constant shear storage modulus (G') in strain sweep experiment with the frequency fixed (1 Hz). Fig. 4A shows how the LVR is shifted to lower strains when the filler content rises while neat epoxy formulation maintain a practically constant G' in all the strain range tested, a Newtonian behavior as expected for the unfilled resin. Filled mixtures found a critical strain above which the structure starts to breakdown earlier when the amount of filler increases [25].

The complex viscosity $|\eta^*|$ of unfilled resin (Fig. 4B) presents an almost constant value on varying the frequency, and a low frequency dependence for the mixture with 10 wt% of BN which could be considered as a dilute solution. However, upon adding 20 wt% of filler or more, the complex viscosity becomes more dependent on the applied frequency, resulting in a more pronounced low frequency shear thinning response typical of layered particles mixtures [26], indicating a significant change in their microstructure. The shear thinning is the decrease of viscosity with the angular frequency that is determined by the balance of hydrodynamic forces, which tends to align the particles with the flow, and rotary Brownian motion that tends to randomize the orientation [27]. It is worth to note, that the increase of $|\eta^*|$ exceeds more than four orders of magnitude on adding 40% wt of BN to the formulation. In addition, an apparent increase of this value is observed in the dilute mixtures, when frequency exceeded a certain critical value, which is associated with the device inertia. The significant change in the microstructure can also be evaluated by the study of storage modulus (G') and loss modulus (G''), which determine the elastic and viscous properties, respectively. Figure 5 shows how on increasing the BN content, the slope of G'

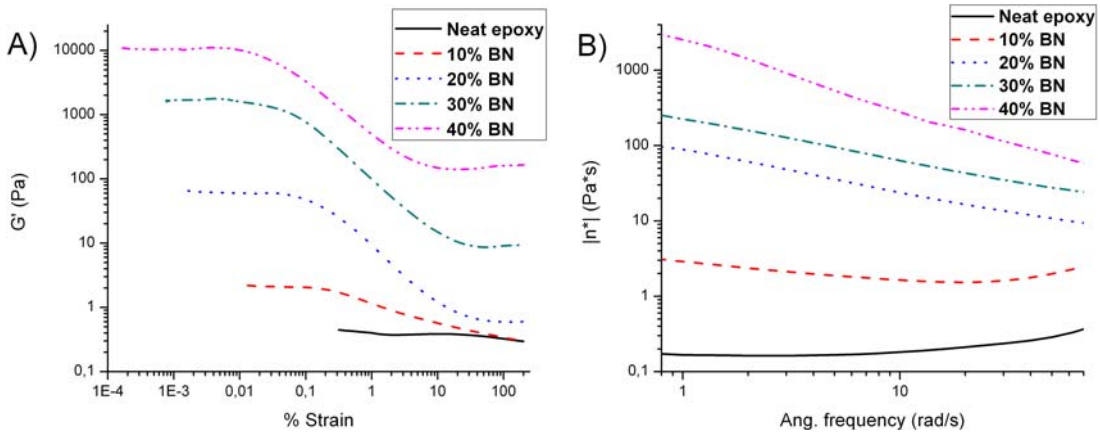

COLOR ONLINE AND BW IN PRINT

FIG. 4. (A) Plot of log G' *versus* log % strain in oscillatory experiments (1 Hz). (B) Plot of log η^* versus log ω, both at 30°C for all the uncured formulations studied. [Color figure can be viewed at wileyonlinelibrary.com]

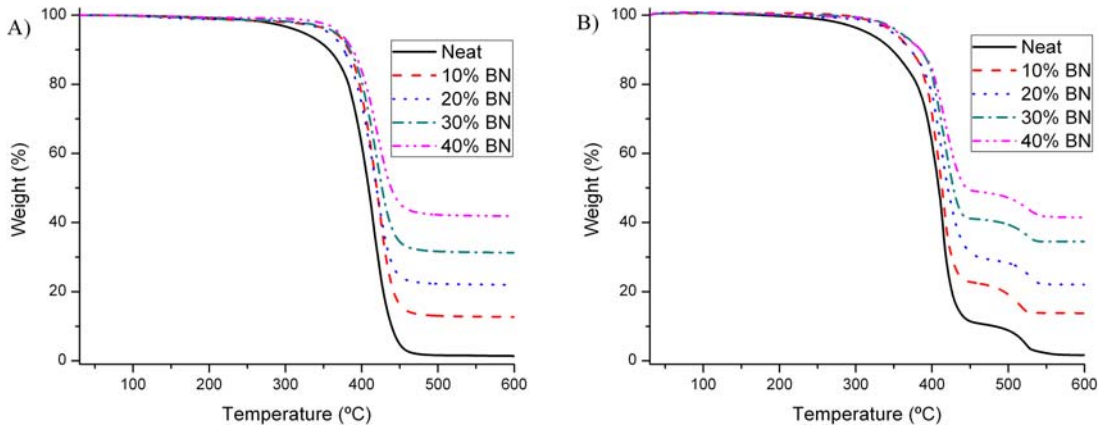

FIG. 6. (A) TGA plots of samples under N_2 atmosphere and (B) under synthetic air. [Color figure can be viewed at wileyonlinelibrary.com]

decreases transforming it to a nearly constant value, independent of the angular frequency, with the addition of 40 wt% of BN.

Also, the change in the liquid like behavior ($G' < G''$) to solid like ($G' > G''$) is observed. This change in the storage modulus at about 20% of BN, with a kind of plateau at low frequency, means that the filled mixture has reached the rheological percolation. Near the percolation threshold (the point in which a pathway of interconnected particles that extends throughout the network is formed) the theory predicts a power law ratio that can be used at a fixed low frequency to determine it [28, 29]:

$$G' \propto (m - m_C)^{\beta} \quad (1)$$

where G' is the storage modulus, m is the mass fraction of BN composites, m_C is the mass fraction at rheological percolation and β is the critical exponent. This relation is often valid only on a very narrow concentration region [7]. The rheological percolation at 1 rad/s was calculated to be 14.4 wt % of BN and the critical exponent 0.84. It should be commented, that the percolation of BN particles in DGEBA formulations was reached at an only 6.9 wt %.

Thermal and Thermomechanical Characterization of the BN Composites

The contribution of BN particles to the composite's behavior was evaluated through different techniques such as TGA, DMTA, and TMA and compared with the neat epoxy matrix.

TGA analyses under inert atmosphere showed an only degradation step (Fig. 6A) and the most representative data are collected in Table 4. The values show a great increase of the temperature of 2% of weight loss on increasing the proportion of filler in the material, about 70°C in reference to the neat epoxy on adding 40% of BN because of the increasing proportion of the inorganic filler and a possible stabilization of the matrix by filler–polymer chain interactions. Moreover, the temperature of maximum degradation rate is kept constant which indicates that the degradation mechanism is not affected by the presence of BN. It is worth mentioning that the char residues are in agreement with the percentages of BN in the composites, since the aliphatic nature of ECC leads to a scarce residue after the complete degradation.

TGA curves registered under air presents two steps (Fig. 6B). The first one related to the thermal degradation process and the second one to the oxidative process. Practically, the same char residue is found in both nitrogen and air. This is due to the fact that the obtained polymer network has the possibility to completely degrade both in inert and oxidizing atmospheres because of the aliphatic structure. The same trend of stabilization effect by BN particles is observed.

By DMTA analysis, we observed the effect of the particles in the mechanic behavior of the cured materials and evaluated the glass transition temperatures of the composites, which could not be easily determined by DSC due to the high crosslinking density of the network which minimize ΔCp. Figure 7A shows the evolution of storage modulus (E') and Fig. 7B shows the evolution of the loss factor tan δ with temperature. It can be observed that the

TABLE 4. Thermogravimetric data of thermosets with several BN contents in N_2 atm.

% BN (in weight)	$T_{2\%}$[a] (°C)	T_{max}[b] (°C)	Char Yield[c] (%)
0	273	415	1
10	298	417	13
20	310	418	22
30	315	419	31
40	342	420	42

[a]Temperature of 2% of weight loss.
[b]Temperature of the maximum decomposition rate.
[c]Char residue at 600°C.

DOI 10.1002/pc

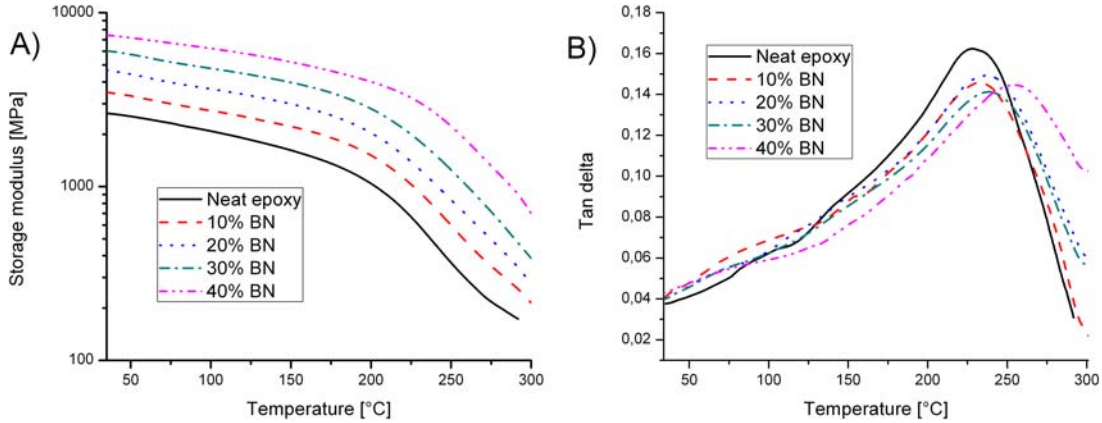

FIG. 7. (A) Storage modulus and (B) tan δ against temperature of the different materials prepared. [Color figure can be viewed at wileyonlinelibrary.com]

relaxation process takes place at high temperatures and this prevented us from determining the modulus after relaxation, since at 300°C the materials were still relaxing but degradation would have already started. Table 5 collects the main parameters extracted from the thermomechanical study.

In Fig. 7B and Table 5 it can be seen that the glass transition temperatures follow an increasing tendency on increasing the filler proportion until temperatures higher than 250°C are reached, extremely large for this type of matrix with an ester group in the network structure, which may undergo β-elimination processes. Similar T_g values were found by Sangermano et al. [30] with the same ECC photochemically cured but very different compared with samples obtained by cationic homopolymerization with lanthanide triflates, which were not higher than 150°C [13]. The tan δ curves in Fig. 7B are very broad indicating a slow relaxation process and have a low intensity indicating low homogeneity in the network structure due the high crosslinking density and to the inherent inhomogeneity caused by the ring-opening polymerization mechanism [3]. The shift of the tan δ peak with increasing BN content indicates there is an interaction between the polymer matrix and the particles further reducing the mobility of the network structure. The increase of Young modulus, although it was not the aim of the present study, reached a 160% of improvement thanks to the reinforcement role of the filler that will be beneficial for the material resistance and its durability.

By TMA, CTE's were measured to assess the dimensional stability of the materials. It can be seen that the addition of filler reduces by >50% this value, which could be favorable for the purposes required in electronic industry. These thermosets usually cover metallic or ceramic substrates with a lower CTE than the polymers and the smaller the difference between their coefficients, the lower internal stresses will be as the working temperature changes leading to a lower thermal fatigue [31].

TABLE 5. Thermomechanical data for the thermosets with different BN content.

% BN (w/w)	Young's modulus[a] (GPa)	$T_{\tan\delta}$[b] (°C)	CTE[c] ($10^{-6}\cdot K^{-1}$)
0	2.4	227	115
10	3.2	232	65
20	4.1	237	66
30	5.1	240	59
40	6.5	254	55

[a]Young's modulus determined by DMTA at 30°C using three-point bending clamp.
[b]Temperature of maximum of tan δ at 1 Hz.
[c]Coefficient of thermal expansion in the vitreous state determined by TMA, between 50 and 75°C.

Mechanical Characterization and Morphology

Coatings applications for electronic devices require a high hardness to keep good appearance of the surface and the protective capacity. To evaluate the resistance against penetration by a static force, we performed microindentation tests. The results obtained using a Knoop microindenter are given in Table 6. It is observed that as the amount of BN increases, the hardness of the composite increases, reaching a maximum value of 26.6 KHN, more than twice the neat matrix.

Adhesion is a complex property that depends on many different factors such as the properties of the coatings and substrates, interfacial interactions or environmental conditions. In addition, differences in CTE's between substrate and coating can lead to the reduction of the adhesion, especially for epoxy cured at high temperature, since the final decrease of temperature after curing creates internal stresses that leads to the production of microcracks or warping. Table 6 shows the apparent shear strength values on steel surfaces for the different materials prepared with different BN content. It can be seen that the shear

TABLE 6. Mechanical properties of the neat materials and composites.

% BN (w/w)	KHN[a]	τ^b (MPa)
0	11.7 ± 0.58	2.34 ± 0.46
10	15.3 ± 0.57	3.11 ± 0.47
20	18.8 ± 0.76	7.58 ± 0.66
30	22.0 ± 0.90	10.65 ± 0.89
40	26.6 ± 1.03	9.96 ± 0.44

[a]Knoop microindentation hardness.
[b]Apparent lap-shear strength over steel surface.

strength increases with the BN content until reached a maximum with the 30% of BN. The reduction of adherence with 40% of BN is related to the diminution of epoxy content. When comparing the observed trends of these properties with those previously reported in DGEBA composites, a different behavior was observed, since the microhardness was only slightly improved and the adhesion remained constant up to 15% of BN content and then decreased [7].

Fracture surfaces were examined by ESEM microscopy. In Fig. 8 it can be clearly observed the phenomenon of the percolation in the transition from 10 to 20% of BN in the material, since the isolated particles in the 10% BN sample collapse in the 20% BN composite. Moreover, in the transition from the neat material to the filled samples it can be seen that the fairly well defined fracture lines in the neat material are transformed into tortuous fracture cracks because of the plans of the BN particles that deviate them, producing the consequent enhancement in toughness.

XRD Diffraction

The XRD is a powerful technique to study the internal structure of materials and to determine the degree of crystallinity of semicrystalline polymers. Figure 9A shows the spectrum of the filler used in the study and the peaks correspond exactly to the hexagonal structure pattern of the BN in the database (01–073-2095 (A)).

The composite with 40 wt% (Fig. 9B) was also analyzed. All the peaks related to BN powder are maintained but they show a small widening due to the presence of resin. It is worth mentioning that a wide peak is observed around 17° of 2Θ due to the amorphous structure of the polymer.

Thermal Conductivity and Electrical Resistivity

The main goal of this research was to improve thermal conductivity of a cycloaliphatic epoxy thermoset by the addition of BN without negatively affect the electrical insulation. Different materials with increasing BN content were investigated by thermal conductivity analysis. The values obtained are represented in Fig. 10. As we can see, the thermal conductivity of the neat resin is highly improved with the increase of BN content. For the sample with 40 wt% of BN (26.0 vol%) the thermal conductivity reaches 1.04 W/m·K, implying an increase of >800%. Chiang and Hsieh obtained similar values of thermal conductivity by using a cycloaliphatic-anhydride system with 25.7 vol% of BN as filler [6]. In addition, a larger increase is observed once percolation is reached. In the previous study on DGEBA composites, a maximum value of 0.61 W/m·K was reached with a 20% wt of BN [7].

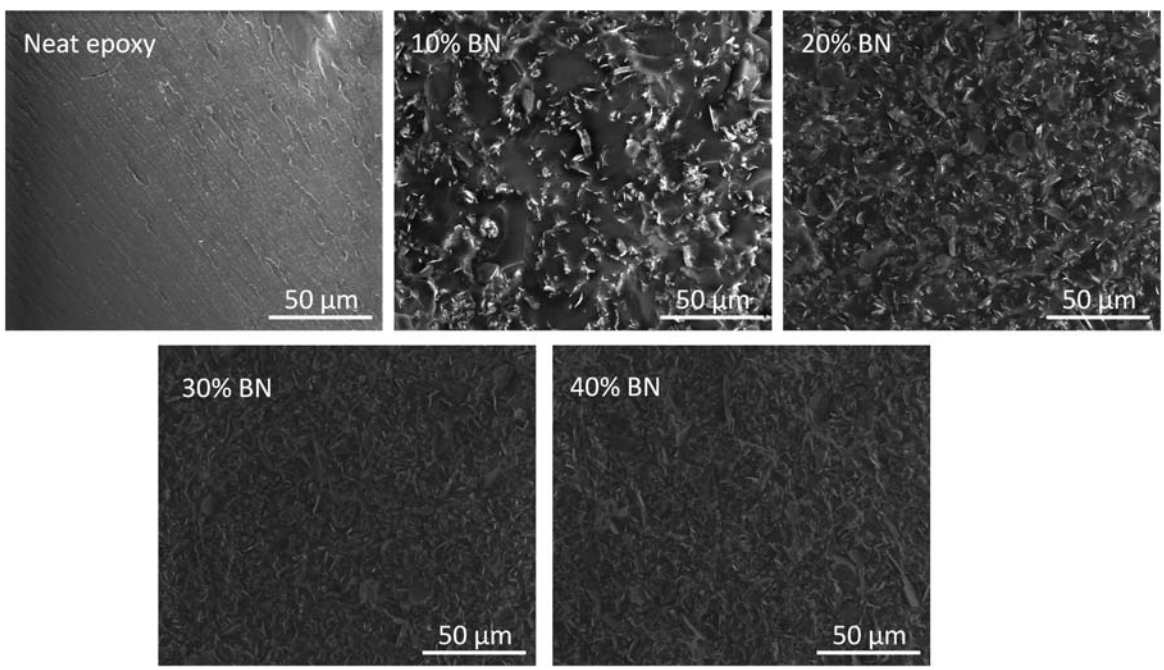

FIG. 8. ESEM micrographs of the fracture surfaces of materials at 800 magnifications.

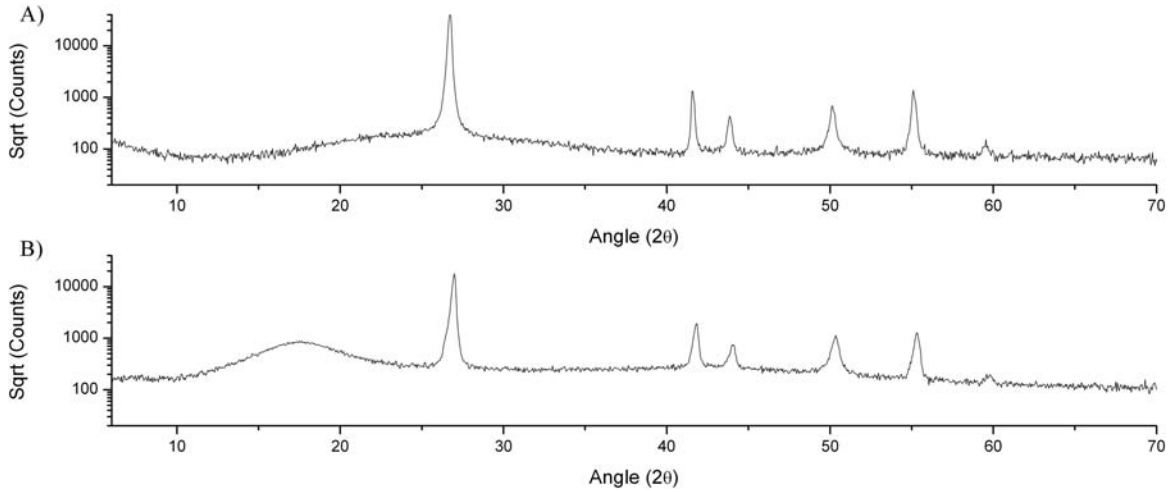

FIG. 9. (A) XRD diffractogram of h-BN particles and (B) 40 wt% composite.

Therefore, our hypothesis that the lower viscosity of ECC allows to reach a higher thermal conductivity, because of the possibility to increase the BN % is confirmed. It should be mentioned, however, that in the literature it can be found references for similar BN contents that reach much higher conductivities [32, 33]. Differences in the curing procedure (using pressure for example), the size and shape of particles, their surface area, and so forth, play a very important role in the increase of thermal conductivity.

Another important parameter in electronic fabrication is the electrical resistance of the thermoset, which quantify the opposition to the current flow. In Fig. 10 the resistivity of each material, resulting of the appliance of 500 V during one minute to the samples, are represented. All the results obtained are over 10^8 Ω·m, enough for electronic industry and they do not depend on the content of BN as other authors have found for electrical conductivity [34].

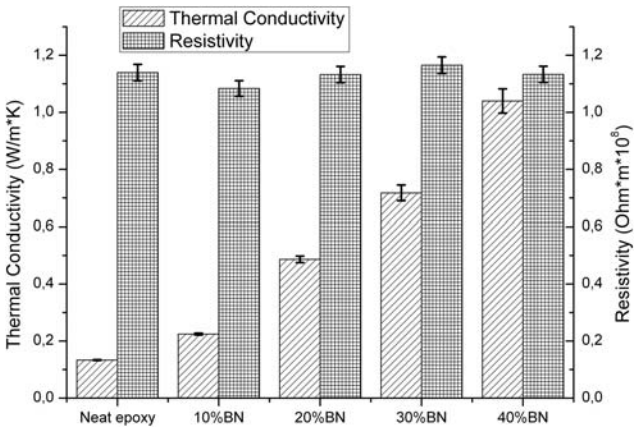

FIG. 10. Thermal conductivity and electric resistivity of the materials prepared on varying the proportion of BN. [Color figure can be viewed at wileyonlinelibrary.com]

CONCLUSIONS

A new latent cationic curing system for ECC was optimized using 1 phr of a benzylammonium salt with 0.1 phr of TEA. This system allows the curing to proceed very quickly on reaching temperatures about 120°C and the formulation can be stored for more than 4 month at room temperature without appreciable change. The addition of BN particles did not lead to any effect on the latency.

By rheological studies we saw an increasing viscosity of formulations on raising the BN proportion. The percolation threshold at 14.4 wt% of BN proportion was determined.

Glass transition temperatures, by DMTA, are higher than 200°C increasing with the BN proportion. Young moduli followed a similar trend. CTEs decreased >50% on adding the filler, which is beneficial for the reduction of thermal stresses.

Microindentation hardness progressively increased with the BN content but apparent shear strength increased until reaching a maximum value with a 30% of BN in the material.

ESEM allows confirming that the percolation occurred between 10 and 20% of BN content. Because of the higher tortuosity of crack propagation, a more tough fracture can be inferred on increasing the BN content.

Thermal conductivities increased in an 800% with the addition of 40 wt% BN filler. According to all these results, the materials obtained are very promising for thermal management applications and to perform multilayer circuit boards.

ACKNOWLEDGMENTS

The authors would like to thank MINECO ~~(MAT2014-53706-C03-01 and 02)~~ and Generalitat de Catalunya ~~(2014-SGR-67)~~ for the financial support. Xavier F.-F also acknowledges the Serra-Húnter program (Generalitat de Catalunya). Gabriel Benmayor S.A. is acknowledged for giving us the BN used in this work.

REFERENCES

1. H. Chen, V.V. Ginzburg, J. Yang, Y. Yang, W. Liu, Y. Huang, L. Du, and B. Chen, *Prog. Polym. Sci.*, **59**, 41 (2016).
2. X.C. Tong, *Advanced Materials for Thermal Management of Electronic Packaging*. Springer, New York, 616 (2011).
3. J.P. Pascault, H. Sauterau, J. Verdu, R.J.J. Williams (Ed.), *Thermosetting Polymers*. Marcel Dekker, New York (2002).
4. X. Huang, P. Jiang, and T. Tanaka, *IEEE Electr. Insul. Mag.*, **27**, 8 (2011).
5. C.A. May, *Epoxy Resins: Chemistry and Technology*, Marcel Dekker Inc., New York (1988).
6. T.H. Chiang, and T.-E. Hsieh, *J. Inorg. Organomet. Polym. Mater.*, **16**, 175 (2006).
7. I. Isarn, L. Massagués, X. Ramis, A. Serra, and F. Ferrando, *Compos. A*, **103**, 35 (2017).
8. K. Yang, and M. Gu, *Compos. A*, **41**, 215 (2010).
9. X. Huang, P. Jiang, and T. Tanaka, *IEEE Elect. Insul. Mag.*, **27**, 8 (2011).
10. W. Green, *Industrial Photoinitiators. A Technical Guide*. CRC Press, Boca Raton (2010).
11. T. Vidil, F. Tournilhac, S. Musso, A. Robisson, and L. Leibler, *Prog. Polym. Sci.*, **62**, 126 (2016).
12. M. Tokizawa, H. Okada, and N. Wakabayashi, *J. Appl. Polym. Sci.*, **50**, 875 (1993).
13. C. Mas, A. Serra, A. Mantecón, J.M. Salla, and X. Ramis, *Macromol. Chem. Phys.*, **202**, 2554 (2001).
14. S. Nakano, and T. Endo, *Prog. Org. Coat*, **23**, 379 (1994).
15. S. Nakano, and T. Endo, *Prog. Org. Coat*, **28**, 143 (1996).
16. S. Nakano, and T. Endo, *J. Polym. Sci. A Polym. Chem.*, **33**, 505 (1995).
17. J.V. Crivello, and S. Liu, *J. Polym. Sci. A Polym. Chem.*, **38**, 389 (2000).
18. H. Lützen, T.M. Gesing, B.K. Kim, and A. Hartwig, *Polymer*, **53**, 6089 (2012).
19. M. Donnay, S. Tzavalas, and E. Logakis, *Compos. Sci. Technol.*, **110**, 152 (2015).
20. J. Yu, H. Mo, and P. Jiang, *Polym. Adv. Technol.*, **26**, 514 (2015).
21. S. Nakano, and T. Endo, *Prog. Org. Coat.*, **22**, 287 (1993).
22. L. Matejka, P. Chabanne, L. Tighzert, and J.P. Pascault, *J. Polym. Sci. A Polym. Chem.*, **32**, 1447 (1994).
23. M. Tejkl, J. Valis, M. Kaplanová, B. Jasúrek, and T. Syrový, *Prog. Org. Coat*, **74**, 215 (2012).
24. M.R. Kamal, and A. Mutel, *J. Polym. Eng.*, **5**, 293 (1985).
25. T.F. Tadros, *Rheology of Dispersions: Principles and Applications*. Wiley-VCH, Weinheim, 76 (2010).
26. J. Ren, and R. Krishnamoorti, *Macromolecules*, **36**, 4443 (2003).
27. C.W. Macosko, R.G. Larson, *Rheology: Principles, Measurements, and Applications*. Wiley-VCH, New York, 440 (1994).
28. G. Hu, C. Zhao, S. Zhang, M. Yang, and Z. Wang, *Polymer*, **47**, 480 (2006).
29. P.G. De Gennes, *J. Phys.*, **37**, 1445 (1976).
30. M. Sangermano, Y. Yagci, and G. Rizza, *Macromolecules*, **40**, 8827 (2007).
31. D.D.L. Chung, L. Li, *Materials for Electronic Packaging*. Butterworth-Heinemann, Newton, 168 (1995).
32. A. Rybak, K. Gaska, C. Kapusta, F. Toche, and V. Salles, *Polym. Adv. Technol.*, **28**, 1676 (2017).
33. K. Gaska, A. Rybak, C. Kapusta, R. Sekula, and A. Siwek, *Polym. Adv. Technol.*, **26**, 26 (2015).
34. 4Y.S. Perets, L.Y. Matzui, L.L. Vovchenko, Y.I. Prylutskyy, P. Scharff, U. Ritter, and *J. Mat. Sci.*, **49**, 2098 (2014).